2018 European Control Conference (ECC)
June 12-15, 2018. Limassol, Cyprus

Voltage Stabilization in a DC MicroGrid by an ISS-like Lyapunov Function implementing Droop Control

Alessio Iovine, Gilney Damm, Elena De Santis
Maria Domenica Di Benedetto, Lilia Galai-Dol, Pierdomenico Pepe

***Abstract*— The interconnection of renewable energy sources with storage systems through a Direct Current (DC) MicroGrid is one of the best ways to deal with the need for reliable power networks. An approach based on the "System of Systems" philosophy using distributed control methodologies is developed here with the purpose to share the duty to ensure grid voltage stability among a number of devices ensuring fast response. The closed-loop stability proof is based on an Input-to-State-Stable (ISS) like Lyapunov function.**

***Abstract*— Voltage control, Lyapunov methods, Input-to-State Stability, DC MicroGrid, Droop control**

I. Introduction

Recently the use of Direct Current (DC) MicroGrids has grown significant interest mainly due to some advantages over Alternate Current (AC) ones [1]. Indeed, DC grids favour the integration of renewable energy sources (renewables), especially photovoltaic (PV), storages as batteries or supercapacitors, and modern loads as electric vehicles due to the DC nature of these devices. The two kinds of storages usually work at different time scales: the batteries have the duty to provide energy when it is missing from the renewable sources, while the supercapacitors act to compensate the power transient variations in power production or consumption [2], [3], [4], [5].

To be able to exchange power in a reliable way, DC grid voltage stability must be ensured under adverse circumstances [6]. To reduce losses due to high currents and to add redundancy to the system, the utilization of more than one storage device is favourable both for batteries and supercapacitors. The combination of the storage devices is usually controlled in a master-slave or droop control framework, according to the number of devices that are dedicated to operate the voltage stabilization (one or more than one, respectively) [7]. Rigorous analysis of voltage stabilization is an open research problem [2], [8], [9], [10], and the result introduced in this paper is among the first ones for droop control of DC MicroGrids.

The target of this paper is to introduce a stability analysis for a DC MicroGrid where more devices share the responsibility to correctly operate the voltage stabilization. To this purpose, the analysis of a DC MicroGrid with a single supercapacitor introduced in [2], which results in a master-slave control, is here extended for a DC MicroGrid with two supercapacitors sharing the duty to stabilize the grid. The master-slave distributed nonlinear control technique presented in [2] is modified into a droop control one, which is obtained by an Input-to-State-Stable (ISS) like Lyapunov function [11] with respect to the equilibrium point playing the role of a (fictitious) input. The here adopted nonlinear techniques result in a less complicated and then more suitable for implementation control law, with respect to the structure it would have using the techniques adopted in [2]. The resulting control law allows for a Lyapunov-based sharing of the needed power to stabilize the grid by different devices with the same target.

This paper is organized as follows. In Section II the model of the DC MicroGrid is introduced. Then in Section III the adopted analysis is carried out for each subsystem to satisfy stability requirements. Section IV provides simulation results, while in Section V conclusions are outlined.

II. MicroGrid configuration

The considered framework in Fig. 1 depicts the DC microgrid with a PV array, a battery, a load and two supercapacitors. To ensure voltage stability and power balance, the control objective is split into several targets. The PV array is controlled in a way such to extract the maximum available power, while the battery acts as a buffer between the power flow requested by the load and the power flow supplied by the renewables, i.e. the PV array. The two supercapacitors share the duty to keep the voltage at a desired level during the transients. The devices are taken as voltage sources, and they are connected to the DC grid by DC/DC converters, whose dynamics are supposed to be measurable, and the values of the electrical components (resistances, capacitances and inductances) are known. The controllers developed in this work are the duty cycles for the DC/DC converters.

A. Assumptions

To ensure voltage stability and power balance, some assumptions need to be made.

First, the existence of a higher level controller which provides references to be accomplished by the local controllers is supposed [12]. These references are about the desired voltages to be imposed to the PV array and to the battery, V_1^* and V_4^* respectively, to obtain the needed amount of power and the desired voltage value for the DC grid, which is V_{11}^*.

Alessio Iovine and Lilia Galai-Dol are with Efficacity, R&D Institute for Urban Energy Transition, Paris, France.
Email: {a.iovine, l.galai-dol}@efficacity.com
Gilney Damm is with IBISC - Paris-Saclay University, Evry, France, and with Efficacity, R&D Institute for Urban Energy Transition, Paris, France. Email: gilney.damm@ibisc.fr
Elena De Santis, Maria Domenica Di Benedetto and Pierdomenico Pepe are with University of L'Aquila, L'Aquila, Italy. Email: {elena.desantis, mariadomenica.dibenedetto, pierdomenico.pepe}@univaq.it

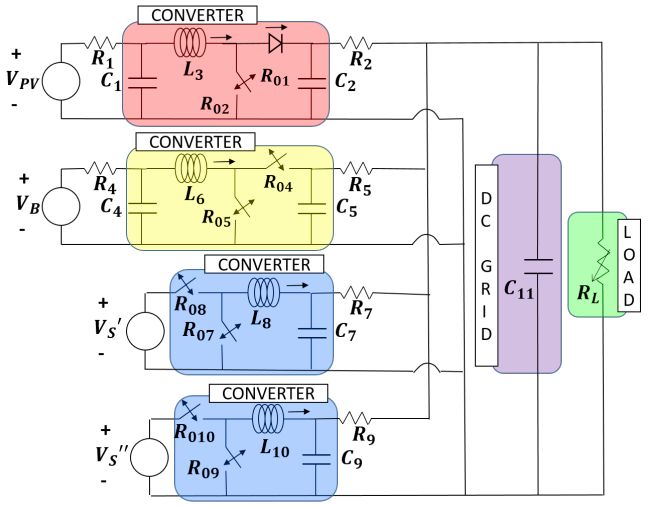

Fig. 1. The considered framework.

We need the references to be able to take into account a proper charge/discharge rate power for the supercapacitors; a state of charge about 50% of its operability (i.e. about 75% of its maximum charge) at the beginning of the time interval is the best starting point for efficiency reasons [13].

Then, proper sizing of each component in a DC microgrid is considered in order to always satisfy the power demanded by the load. This condition can also be seen as the ability of the battery and the supercapacitors to fulfil the request to provide enough amount of power in a time interval.

Last, the assumption to work in a feasible framework due to physical limitations of the devices, and consequently to deal with loads, disturbances and control gains allowing for a solution, must be made. Then a situation where the system is stabilizable in case of bounded control inputs is considered ($u_i \in [0,1]$, $i = 1,2,3,4$), according to an operating region as the one described in [2].

B. MicroGrid Modeling

The PV array, battery and supercapacitors are each one connected to the DC grid by a DC/DC converter. Here the mathematical models are given according to the circuital representation, based on power electronics averaging technique controlled using Pulsed Width Modulation (PWM) [14].

The considered model is

$$\dot{x}(t) = f(x(t)) + g(x(t), u(t), d(t)) + h(x(t), d(t)) \quad (1)$$

$$x = [\ x_1\ \ x_2\ \ x_3\ \ x_4\ \ x_5\ \ x_6\ \ x_7\ \ x_8\ \ x_9\ \ x_{10}\ \ x_{11}\ ]^T \quad (2)$$

$$u = [\ u_1\ \ u_2\ \ u_3\ \ u_4\ ]^T \quad (3)$$

$$d = \left[\ V_{PV}\ \ V_B\ \ V_S'\ \ V_S''\ \ \frac{1}{R_L}\ \right]^T \quad (4)$$

The state $x \in \mathbb{R}^{11}$ and the disturbance vector $d \in \mathbb{R}^5$ are supposed to be measurable, and the parameters are known. Here x_i represents the voltage $V_{C_i} \in \mathbb{R}^+$ of the capacitor C_i, $i = \{1,2,4,5,7,9,11\}$ while x_j represents the current $I_{L_j} \in \mathbb{R}$ in the inductance L_j, $j = \{3,6,8,10\}$. x_{11} represents the voltage of the DC microgrid, while the other variables are part of the DC/DC converters connecting the voltage sources $V_{PV} \in \mathbb{R}^+$, $V_B \in \mathbb{R}^+$, $V_S' \in \mathbb{R}^+$, $V_S'' \in \mathbb{R}^+$ (the PV array, battery and supercapacitors, respectively) to the DC grid. The control vector u is composed by the duty cycles of the converters. $R_L \in \mathbb{R}^+$ is a piecewise constant value representing the load resistance.

$$\begin{cases}
\dot{x}_1 = \frac{1}{R_1 C_1}(V_{PV} - x_1) - \frac{1}{C_1} x_3 \\
\dot{x}_2 = \frac{1}{R_2 C_2}(x_{11} - x_2) + \frac{1}{C_2} x_3 (1 - u_1) \\
\dot{x}_3 = \frac{1}{L_3} x_1 - \frac{1}{L_3} x_2 (1 - u_1) - \frac{R_{01}}{L_3} x_3 \\
\dot{x}_4 = \frac{1}{R_4 C_4}(V_B - x_4) - \frac{1}{C_4} x_6 \\
\dot{x}_5 = \frac{1}{R_5 C_5}(x_{11} - x_5) + \frac{1}{C_5} x_6 (1 - u_2) \\
\dot{x}_6 = \frac{1}{L_6} x_4 - \frac{1}{L_6} x_5 (1 - u_2) - \frac{R_{04}}{L_6} x_6 \\
\dot{x}_7 = \frac{1}{R_7 C_7}(x_{11} - x_7) + \frac{1}{C_7} x_8 \\
\dot{x}_8 = \frac{1}{L_8} V_S' u_3 - \frac{R_{08}}{L_8} x_8 - \frac{1}{L_8} x_7 \\
\dot{x}_9 = \frac{1}{R_9 C_9}(x_{11} - x_9) + \frac{1}{C_9} x_{10} \\
\dot{x}_{10} = \frac{1}{L_{10}} V_S'' u_4 - \frac{R_{010}}{L_{10}} x_{10} - \frac{1}{L_{10}} x_9 \\
\dot{x}_{11} = \frac{x_2 - x_{11}}{R_2 C_{11}} + \frac{x_5 - x_{11}}{R_5 C_{11}} + \frac{x_7 - x_{11}}{R_7 C_{11}} + \\
\qquad + \frac{x_9 - x_{11}}{R_9 C_{11}} - \frac{x_{11}}{R_L C_{11}}
\end{cases} \quad (5)$$

The voltage of the DC grid x_{11} is influenced by the connection with load and sources. The DC/DC converter connecting the PV array to the DC grid is a boost one and it is illustrated in the red area in Fig. 1. Its target is to obtain the maximum amount of power from the PV array regulating the voltage V_{C_1} to the constant reference $V_1^* = x_1^*$, which is given by the higher level controller implementing the Maximum Power Point Tracking (MPPT) algorithm. u_1 is the corresponding control input. The DC/DC converter connecting the battery is a bost-buck bidirectional converter (yellow area in Fig. 1). Its duty cycle, i.e. u_2, is controlled to assign the constant reference $V_4^* = x_4^*$ value to x_4, to the purpose to force the battery to provide/absorb an already fixed amount of power. The DC/DC converters connecting the supercapacitors to the DC grid are bidirectional buck-boost ones (blue areas in Fig. 1). The duty cycles u_3 and u_4 are the control inputs for each system. Their target is to control the capacitors' voltage directly connected to the grid, x_7 and x_9 respectively, such as to keep the voltage x_{11} at the reference value x_{11}^*. The constant references are supposed correctly given by the higher level controller, as stated in Section II-A.

III. MicroGrid Control

A. Connection with Droop control

The desired target to be accomplished in this work is to provide an analytical result for several network nodes sharing out the responsibility to maintain the DC voltage of the grid at the same time. The necessity to have physical redundancy is considered, and a cooperative solution among two equal stability dedicated devices (the supercapacitors) is investigated. A dedicated control action must be developed when they are grid connected and in operating condition. Indeed, when a power imbalance reaction is needed, the optimal solution would be to have them reacting in the same way for restoring a desired voltage level into the DC grid. The power imbalance can be caused by unmodeled dynamics or disturbances acting on the renewable source or the load.

The control of the grid is based on the construction of an ISS-Lyapunov function, which will also provide the duty of each device to provide/absorb power. The responsibility to keep the voltage will be equally distributed between the dedicated devices: to this purpose, the gain Γ is introduced as $\Gamma = \frac{1}{n}$, where n is the number of the aforementioned devices. In this work $n = 2$ is considered.

It must to be noted that the gain Γ corresponds to the droop gains adopted when performing droop control. It is then possible to state that the performed control action acts according to the droop control mode. The considered case is clearly correlated to equal droop gains, which happens when the devices are equal in size and state of charge. In this paper, the contribution is focused to this particular case due to the complications of the general one with respect to different convergence rates and proper choice of the gains. Target of future works will be to develop an analytical result for devices with different characteristics.

B. Control law

For each DC/DC converter a proper control action is developed to fit the desired target and the interconnection among all of them is then used to ensure grid stability.

Let us consider the set of all possible values of x_1^* that generate a non negative current coming from the PV array as $x_1^* \in [\gamma_1 V_{PV}, V_{PV}]$, where $\gamma_1 = \frac{R_{01}}{R_1}\frac{1}{1+\frac{R_{01}}{R_1}}$. Also, let us consider a value for x_4^* and x_{11}^* such that they do not violate physical constraints of the converter, i.e. $x_4^* \in [\gamma_2 V_B, \beta(x_{11}^*, V_B)]$, where $\gamma_2 = \frac{R_{04}}{R_4}\frac{1}{1+\frac{R_{04}}{R_4}}$,

$$\beta(x_{11}^*, V_B) = \frac{x_{11}^* + \left(\frac{R_5}{R_4} - \frac{R_{04}}{R_4}\right) V_B}{1 + \frac{R_5}{R_4} - \frac{R_{04}}{R_4}} \tag{6}$$

and $x_{11}^*,\ x_{11}^* \in (max(V_{PV}, V_B), min(V_S', V_S''))$. Let us moreover consider the set of all positive values of R_L in the set Ω_{R_L} satisfying the condition on the balance of the currents, which is expressed by

$$\frac{1}{R_L} x_{11}^* = \frac{1}{R_2}(x_2^* - x_{11}^*) + \frac{1}{R_5}(x_5^* - x_{11}^*) \tag{7}$$

where

$$\Omega_{R_L} = \{R_L : x_4^* \in [\gamma_2 V_B, \beta(x_{11}^*, V_B)] \text{ for some } x_1^* \in [\gamma_1 V_{PV}, V_{PV}]\} \tag{8}$$

and the values of x_2^* and x_5^* depend on x_1^* and x_4^*, respectively, and for $i = \{2, 5\}$ are defined as

$$x_i^* = \frac{x_{11}^*}{2} + \frac{1}{2}\sqrt{{x_{11}^*}^2 + 4R_i C_i \Delta_i} \tag{9}$$

$$\Delta_2 = \frac{1}{R_1 C_2}(V_{PV} - x_1^*)\left[x_1^* - \frac{R_{01}}{R_1}(V_{PV} - x_1^*)\right] \tag{10}$$

$$\Delta_5 = \frac{1}{R_4 C_5}(V_B - x_4^*)\left[x_4^* - \frac{R_{04}}{R_4}(V_B - x_4^*)\right] \tag{11}$$

and represent the solution of the dynamics x_2 and x_5 in equation (5) setting $\dot{x} = 0$.

Let us consider the state x, whose dynamics are described in (5), the integral terms α_1, α_3, α_4, α_6 assuring zero error in steady state and the positive gains K_1, $\overline{K}_1$, K_1^α, K_3, $\overline{K}_3$, K_3^α, K_4, $\overline{K}_4$, K_4^α, K_6, $\overline{K}_6$, K_6^α:

$$\dot{\alpha}_1 = K_1^\alpha(x_1 - x_1^*) \ ; \ \dot{\alpha}_3 = K_3^\alpha(x_3 - z_3) \tag{12}$$

$$\dot{\alpha}_4 = K_4^\alpha(x_4 - x_4^*) \ ; \ \dot{\alpha}_6 = K_6^\alpha(x_6 - z_6) \tag{13}$$

where

$$z_3 = \frac{1}{R_1}(V_{PV} - x_1) + C_1 K_1(x_1 - x_1^*) + C_1 \overline{K}_1 \alpha_1 \tag{14}$$

$$z_6 = \frac{1}{R_4}(V_B - x_4) + C_4 K_4(x_4 - x_4^*) + C_4 \overline{K}_4 \alpha_4 \tag{15}$$

Let us define the errors e_2 and e_5 as the differences between x_2 and x_5 and their equilibrium points $x_2^e = x_2^*$, $x_5^e = x_5^*$;

$$e_2 = x_2 - x_2^*, \qquad e_5 = x_5 - x_5^* \tag{16}$$

and the terms

$$\Psi_2 = e_2\left(\frac{1}{R_2}(x_{11} - x_2^*) + x_3(1 - u_1)\right) \tag{17}$$

$$\Psi_5 = e_5\left(\frac{1}{R_5}(x_{11} - x_5^*) + x_6(1 - u_2)\right) \tag{18}$$

$$\Psi_{11} = x_{11}\left(\frac{e_2 + x_2^* - x_{11}}{R_2} + \frac{e_5 + x_5^* - x_{11}}{R_5} - \frac{x_{11}}{R_L}\right) \tag{19}$$

to be used in the references z_i for x_i, $i = \{7, 9\}$, and z_j, $j = \{8, 10\}$, with the positive gains K_i and K_j:

$$z_i = \frac{1}{x_{11}}{x_{11}^*}^2 - \frac{R_i}{x_{11}}\Gamma\left[\Psi_2 + \Psi_5 + \Psi_{11}\right] \tag{20}$$

$$z_j = C_i K_i(x_i - z_i) - \frac{1}{R_i}(x_i - x_{11}) - C_i \dot{z}_i \tag{21}$$

Let us now consider η, where

$$\eta = \begin{pmatrix} x_1 - x_1^* \ ; \ \alpha_1 \ ; \ x_2 - x_2^* \ ; \ x_3 - z_3 \ ; \ \alpha_3 \ ; \\ x_4 - x_4^* \ ; \ \alpha_4 \ ; \ x_5 - x_5^* \ ; \ x_6 - z_6 \ ; \ \alpha_6 \ ; \\ x_7 - z_7 \ ; \ x_8 - z_8 \ ; \ x_9 - z_9 \ ; \ x_{10} - z_{10} \ ; \ x_{11} \end{pmatrix} \tag{22}$$

Finally, let us consider the gain $\Gamma = 0.5$ and the set Ω_η of any evolution of η satisfying for each t the conditions:

$$x_2 \neq 0, \quad x_5 \neq 0, \quad x_{11} \neq 0 \tag{23}$$

Theorem 1. *For any given $x_1^* \in [\gamma_1 V_{PV}, V_{PV}]$, $x_4^* \in [\gamma_2 V_B, \beta(x_{11}^*, V_B)]$, $x_{11}^* \in (max(V_{PV}, V_B), min(V_S', V_S''))$, $R_L \in \Omega_{R_L}$ such that condition (7) is satisfied, there exist control laws u_1, u_2, u_3, u_4 such that, for suitable functions $\omega \in K\mathcal{L}$ and $\gamma \in K$, the following inequality holds*

$$|\eta(t)| \leq \omega(\eta(0), t) + \gamma(x_{11}^*), \tag{24}$$

provided that $\eta \in \Omega_\eta$.

Proof. A Lyapunov function V composed of different Lyapunov functions is used to prove stability, as illustrated in [6], [15], [2]. State-feedback Proportional Integral (PI) control inputs u_1 and u_2 are designed for properly controlling dynamics x_1, x_3, x_4 and x_6 in order to obtain a desired amount of power coming from the PV array and the battery. Then the control inputs u_3 and u_4 are dedicated to the grid voltage regulation for the system interconnection. Backstepping technique is used to implement the control laws. The proposed candidate Lyapunov function is in the form of

$$V(\eta) = V_{1,3} + V_{4,6} + V_{7,9} + V_{8,10} + V_{2,5,11} > 0 \tag{25}$$

Let us consider the equilibrium points $x_1^e = x_1^*$, $x_3^e = \frac{1}{R_1}(V_{PV} - x_1^*)$, $x_4^e = x_4^*$ and $x_6^e = \frac{1}{R_4}(V_B - x_4^*)$. They are necessary to provide power stability, i.e. that the PV array and the battery feed the load in steady state. To prove convergence, the following candidate Lyapunov functions are considered:

$$V_{1,3} = \frac{1}{2}(x_1 - x_1^*)^2 + \frac{\overline{K}_1}{2K_1^\alpha}\alpha_1^2 + \frac{1}{2}(x_3 - z_3)^2 + \frac{\overline{K}_3}{2K_3^\alpha}\alpha_3^2 \tag{26}$$

$$V_{4,6} = \frac{1}{2}(x_4 - x_4^*)^2 + \frac{\overline{K}_4}{2K_4^\alpha}\alpha_4^2 + \frac{1}{2}(x_6 - z_6)^2 + \frac{\overline{K}_6}{2K_6^\alpha}\alpha_6^2 \tag{27}$$

where the positive gains K_1, $\overline{K}_1$, K_1^α, K_3, $\overline{K}_3$, K_3^α, K_4, $\overline{K}_4$, K_4^α, K_6, $\overline{K}_6$, K_6^α, have to be properly chosen. The control inputs u_1 and u_2 are defined as

$$u_1 = \frac{1}{x_2}\left[-x_1 + x_2 + R_{01}x_3 - L_3 v_1\right] \tag{28}$$

$$u_2 = \frac{1}{x_5}\left(-x_4 + x_5 + R_{04}x_6 - L_6 v_4\right) \tag{29}$$

with, for $(i,j) = \{(1,3),(4,6)\}$,

$$\begin{aligned} v_i = {} & K_j(x_j - z_j) + \overline{K}_j\alpha_j - C_i\overline{K}_i K_i^\alpha (x_i - x_i^*) + \\ & + \left(C_i K_i - \frac{1}{R_i}\right)\left(K_i(x_i - x_i^*) + \overline{K}_i\alpha_i\right) \end{aligned} \tag{30}$$

and make negative semidefinite the time derivative of the candidate Lyapunov functions $V_{1,3}$ and $V_{4,6}$;

$$\dot{V}_{1,3} = -K_1(x_1 - x_1^*)^2 - K_3(x_3 - z_3)^2 \leq 0 \tag{31}$$

$$\dot{V}_{4,6} = -K_4(x_4 - x_4^*)^2 - K_6(x_6 - z_6)^2 \leq 0 \tag{32}$$

Asymptotic stability is then proven by $\ddot{V}_{1,3}$ and $\ddot{V}_{4,6}$. Indeed, since $\dot{V}_{1,3} \leq 0$ then $V_{1,3}(t) \leq V_{1,3}(0)$, which implies that $x_1 - x_1^*$, α_1, $x_3 - z_3$ and α_3 are bounded, thanks to Lyapunov theorem. Consequently $\ddot{V}_{1,3}$ is bounded as well. Then $\dot{V}_{1,3}$ is uniformly continuous in time and applying Barbalat's lemma we establish that $\dot{V}_{1,3} \to 0$ as $t \to \infty$: ergo $(x_1 - x_1^*) \to 0$, $\alpha_1 \to 0$, $(x_3 - z_3) \to 0$ and $\alpha_3 \to 0$ [16]. The same is valid for $\dot{V}_{4,6}$ and $\ddot{V}_{4,6}$.

$$\ddot{V}_{1,3} = -2K_1(x_1 - x_1^*)(\dot{x}_1) - 2K_3(x_3 - z_3)(\dot{x}_3 - \dot{z}_3) \tag{33}$$

$$\begin{aligned} \dot{z}_3 = {} & \left(\frac{1}{R_1} - C_1 K_1\right)\left(K_1(x_1 - x_1^*) + \overline{K}_1\alpha_1\right) + \\ & + C_1\overline{K}_1 K_1^\alpha (x_1 - x_1^*) \end{aligned} \tag{34}$$

Then asymptotic stability around the defined equilibrium points is ensured with the previously defined u_1 and u_2. The control inputs u_3 and u_4 are dedicated to ensure grid stability: they do not act directly on the DC grid, but through the dynamics x_8 and x_7 for u_3 and x_{10} and x_9 for u_4. To find a proper control action, $V_{2,5,11}$ is defined as:

$$V_{2,5,11} = \frac{C_2}{2}e_2^2 + \frac{C_5}{2}e_5^2 + \frac{C_{11}}{2}x_{11}^2 \tag{35}$$

where the errors e_2 and e_5 are defined in (16). The corresponding dynamical equations are rewritten as

$$\begin{cases} \dot{e}_2 = \frac{1}{R_2 C_2}(x_{11} - e_2 - x_2^*) + \frac{1}{C_2}x_3(1 - u_1) \\ \dot{e}_5 = \frac{1}{R_5 C_5}(x_{11} - e_5 - x_5^*) + \frac{1}{C_5}x_6(1 - u_2) \\ \dot{x}_{11} = \frac{1}{C_{11}}\left(\frac{1}{R_2}(e_2 + x_2^* - x_{11}) + \frac{1}{R_5}(e_5 + x_5^* - x_{11})\right) + \\ \quad + \frac{1}{C_{11}}\left(\frac{1}{R_7}(x_7 - x_{11}) + \frac{1}{R_9}(x_9 - x_{11}) - \frac{1}{R_L}x_{11}\right) \end{cases} \tag{36}$$

and the time derivative $\dot{V}_{2,5,11}$ of (35) is

$$\begin{aligned} \dot{V}_{2,5,11} = {} & -\frac{1}{R_2}e_2^2 - \frac{1}{R_5}e_5^2 + \Psi_2 + \Psi_5 + \Psi_{11} + \\ & + x_{11}\left(\frac{1}{R_7}(x_7 - x_{11}) + \frac{1}{R_9}(x_9 - x_{11})\right) \end{aligned} \tag{37}$$

In equation (37) the dynamics x_7 and x_9 are the virtual control input; properly selected, they will give the desired form to $\dot{V}_{2,5,11}$. With $\Gamma = 0.5$, it is then possible to write the references z_i for x_i, $i = \{7, 9\}$ in (20) such to have a $\dot{V}_{2,5,11}$ in a proper form for ISS (the explication is at the end of the proof):

$$\dot{V}_{2,5,11} = -\frac{1}{R_2}e_2^2 - \frac{1}{R_5}e_5^2 - R_e x_{11}^2 + R_e {x_{11}^*}^2 \tag{38}$$

where $R_e = \left(\frac{1}{R_7} + \frac{1}{R_9}\right)$. The references z_j, $j = \{8, 10\}$ in (21) are then calculated in order to ensure convergence. Indeed, the dedicated positive definite Lyapunov function $V_{7,9}$ is shown to have a definite negative time derivative:

$$V_{7,9} = \frac{1}{2}(x_7 - z_7)^2 + \frac{1}{2}(x_9 - z_9)^2 \tag{39}$$

$$\dot{V}_{7,9} = -K_7(x_7 - z_7)^2 - K_9(x_9 - z_9)^2 < 0 \quad (40)$$

Finally the control inputs u_3 and u_4 are defined as

$$u_3 = \frac{1}{V_S'}\left[x_7 + R_{08}x_8 + L_8\dot{z}_8 - L_8K_8(x_8 - z_8)\right] \quad (41)$$

$$u_4 = \frac{1}{V_S''}\left[x_9 + R_{010}x_{10} + L_{10}\dot{z}_{10} - L_{10}K_{10}(x_{10} - z_{10})\right] \quad (42)$$

with $K_8 > 0$ and $K_{10} > 0$ constant, and where $\dot{z}_8$, $\dot{z}_{10}$ are the time derivatives of z_8 and z_{10}, respectively. Then, the positive definite Lyapunov function $V_{8,10}$ has a negative definite time derivative $\dot{V}_{8,10}$.

$$V_{8,10} = \frac{1}{2}(x_8 - z_8)^2 + \frac{1}{2}(x_{10} - z_{10})^2 \quad (43)$$

$$\dot{V}_{8,10} = -K_8(x_8 - z_8)^2 - K_{10}(x_{10} - z_{10})^2 < 0 \quad (44)$$

According to (26), (27), (35), (39), (43), it is then possible to state that

$$\underline{\alpha}(|\eta|) \leq V(\eta) \leq \overline{\alpha}(|\eta|) \quad (45)$$

where the functions $\overline{\alpha}, \underline{\alpha} \in K_\infty$. Furthermore, from the conditions in (31), (32), (38), (40) and (44) it follows that there exist functions $\alpha, \overline{\gamma} \in K_\infty$ such that the following equality/inequality holds:

$$\begin{aligned}\dot{V}(\eta, x_{11}^*) &= \dot{V}_{1,3} + \dot{V}_{4,6} + \dot{V}_{7,9} + \dot{V}_{8,10} + \dot{V}_{2,5,11} \quad (46)\\ &\leq -\alpha(|\eta|) + \overline{\gamma}(|x_{11}^*|)\end{aligned}$$

The composite positive definite Lyapunov function $V(\eta)$ in (25) then results to be an ISS-like Lyapunov function (see page 16 of [11]) with the equilibrium point x_{11}^* playing the role of a (fictitious) input. From (46) the inequality (24) follows, provided that $\eta \in \Omega_\eta$.

□

In Theorem 1, the unconstrained controllers u_1, u_2, u_3 and u_4 locally solve the problem to effectively stabilize a DC microgrid implementing the proposed control method. When considering the bounds on the control inputs we need to compute the maximal set $\Omega_K \subset X$, $X = \mathbb{R}^{15}$ being the state of the closed loop system, which is invariant for the closed loop dynamical system, and such that $u_1(\eta) \in [0, 1]$, $u_2(\eta) \in [0, 1]$, $u_3(\eta) \in [0, 1]$, $u_4(\eta) \in [0, 1]$, $\forall\, \eta \in \Omega_K$. Such a maximal set is well defined, because the family of all invariant sets in X is closed under union. In [2] the set Ω_K is shown not to be empty and suggestions for finding an estimation of it are introduced. Then Theorem 1 is valid also for bounded inputs $u_i \in [0, 1]$, $i = 1, 2, 3, 4$, provided that the initial states are in Ω_K.

It must to be noticed that the control law u_1 and u_2 are similar with respect to the ones introduced in [2], since they perform the same target: nevertheless, the nonliner techniques used in this proof better explain the physical meaning of the equations. On the contrary, the control laws with voltage stability as target have different structures due to the coupling of the control inputs and to the fact that the references (20) are obtained with a different technique, which is ISS. The choice of ISS has been done to simplify the control law.

TABLE I

GRID PARAMETERS.

Param.	Value	Param.	Value	Param.	Value
C_1	0.1 F	C_2	0.01 F	L_3	0.033 H
R_{01}	0.01 Ω	R_{02}	0.01 Ω	R_1	0.1 Ω
R_2	0.1 Ω	C_4	0.1 F	C_5	0.01 F
L_6	0.033 H	R_{04}	0.01 Ω	R_{05}	0.01 Ω
R_4	0.1 Ω	R_5	0.01 Ω	C_7	0.01 F
L_8	0.0033 H	R_{07}	0.01 Ω	R_{08}	0.01 Ω
R_7	0.1 Ω	C_9	0.01 F	L_{10}	0.0033 H
R_{09}	0.01 Ω	R_{010}	0.01 Ω	R_9	0.1 Ω
C_{11}	0.0001 F	F	5 kHz		

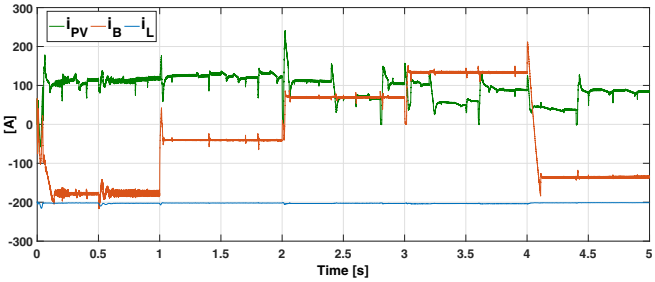

Fig. 2. The current produced by the PV array (i_{PV}), the current absorbed/provided by the battery (i_B) and the current consumed by the load (i_L).

IV. SIMULATION RESULTS

In this Section, simulations showing the results obtained using the proposed control method are introduced. They are performed with SimPower, a Matlab/Simulink toolbox dedicated to realistic circuit simulations. The values of the parameters for the model are depicted in Tables I. The considered simulation time is 5 s.

In the considered scenario a time-varying irradiance profile will generate perturbations coming from the PV array and acting on the DC grid, as shown by the current coming from the PV array in Fig. 2.

During the simulation time the references x_1^* and x_4^* take a different value every second (see Fig. 3), while x_{11}^* is kept constant at the desired value of 1000 V (see Fig. 6). Fig. 3 illustrates the effectiveness of the control action implemented by u_1 and u_2; indeed, the dynamics reach the desired values and keep it even in presence of disturbances, correctly generating the currents i_{PV} and i_B of Fig. 2.

As can be deduced comparing power in and power out in Fig. 2, an action to ensure power balance is requested to the two supercapacitors, both during the transient time than in

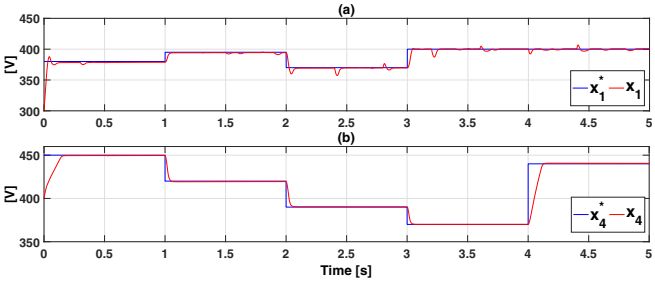

Fig. 3. The voltages x_1 (in (a)) and x_4 (in (b)) and their reference values changing during the considered time intervals of 1 s.

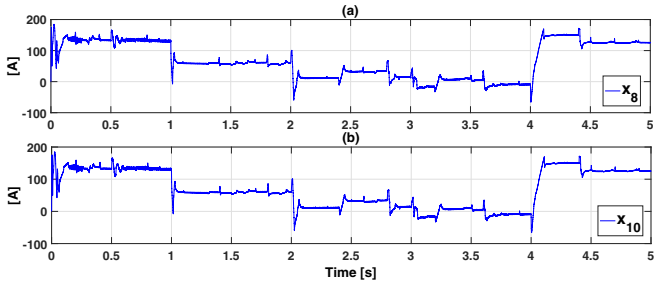

Fig. 4. The currents x_8 and x_{10} provided by the two supercapacitors

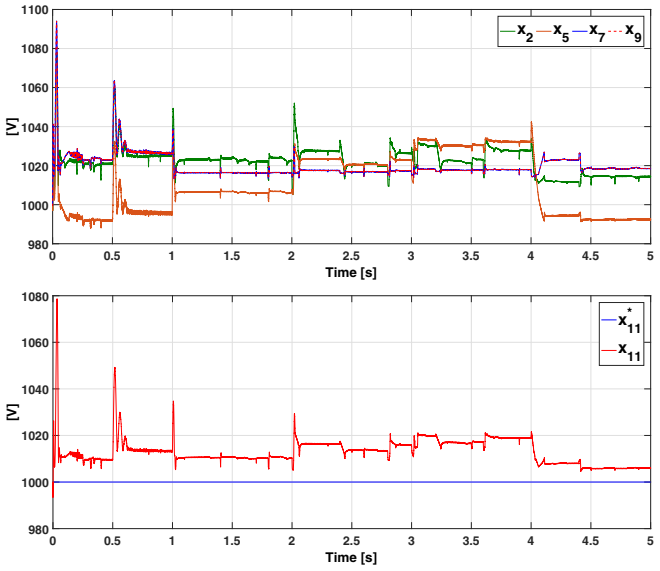

Fig. 6. The DC grid voltage x_{11} and its reference x_{11}^*.

steady state. The developed control laws u_3 and u_4 equally share this responsibility between the two devices thanks to the equal choice of the droop-like gain Γ. As a consequence, the currents generated by the two devices must to be equal, as shown by Fig. 4. Such equal currents also generate the same voltage variations in the dynamics x_7 and x_9, as shown in Fig. 5.

The introduced distributed coupled control action reach the target to maintain the grid voltage around the desired equilibrium point, as shown in Fig. 6. Without considering the high peak taking place during system initialization, which is still under the admissible tolerance of 10%, the system response to the different kinds of disturbances is very appropriate. Indeed, the voltage level is kept with an acceptable error which is less than 5%. The developed distributed controller is then shown to successfully reach the target to control DC grid voltage stability under different adverse circumstances.

V. Conclusions

In this paper an ISS-Lyapunov based distributed control for a DC MicroGrid composed by a PV array, two kinds of storage devices, a load and their connected devices is introduced. The DC MicroGrid is controlled in order to correctly provide a desired amount of power for feeding an uncontrolled bounded load while ensuring a desired grid voltage value. To this purpose, a Lyapunov-based stability analysis is carried out for the complete system; the introduced Lyapunov function is used for sharing the needed power exchange between the two devices providing transient stability in a droop control like mode, supposing enough availability of power for long term stability. Finally, the efficiency of the proposed control is shown by realistic simulation results.

Future works will investigate a more general "Plug and Play" scenario [10] with scalability of the proposed techniques as main target, integrating a number of sources as renewables, a number of storages acting as energy reservoirs and a number of storages acting as power reservoirs. It will also be studied how to design the droop gains as a function of the desired operation regions and performances.

References

[1] L. E. Zubieta, "Are microgrids the future of energy?: DC microgrids from concept to demonstration to deployment," *IEEE Electrification Magazine*, vol. 4, no. 2, pp. 37–44, 2016.

[2] A. Iovine, S. B. Siad, G. Damm, E. D. Santis, and M. D. D. Benedetto, "Nonlinear control of a dc microgrid for the integration of photovoltaic panels," *IEEE Transactions on Automation Science and Engineering*, vol. 14, pp. 524–535, April 2017.

[3] A. Iovine, S. B. Siad, G. Damm, E. D. Santis, and M. D. D. Benedetto, "Nonlinear control of an AC-connected DC MicroGrid," in *IECON 2016 - 42nd Annual Conference of the IEEE Industrial Electronics Society*, pp. 4193–4198, Oct 2016.

[4] R. F. Bastos, T. Dragicevic, J. M. Guerrero, and R. Q. Machado, "Decentralized control for renewable dc microgrid with composite energy storage system and uc voltage restoration connected to the grid," in *IECON 2016 - 42nd Annual Conference of the IEEE Industrial Electronics Society*, pp. 2016–2021, Oct 2016.

[5] G. Fiore, A. Iovine, E. De Santis, and M. D. Di Benedetto, "Secure state estimation for DC microgrids control," in *2017 13th IEEE Conference on Automation Science and Engineering (CASE)*, pp. 1610–1615, Aug 2017.

[6] P. Kundur, J. Paserba, V. Ajjarapu, G. Andersson, A. Bose, C. Canizares, N. Hatziargyriou, D. Hill, A. Stankovic, C. Taylor, T. Van Cutsem, and V. Vittal, "Definition and classification of power system stability IEEE/CIGRE joint task force on stability terms and definitions," *Power Systems, IEEE Transactions on*, vol. 19, pp. 1387–1401, Aug 2004.

[7] T. Dragicevic, J. Vasquez, J. Guerrero, and D. Skrlec, "Advanced LVDC Electrical Power Architectures and Microgrids: A step toward a new generation of power distribution networks.," *Electrification Magazine, IEEE*, vol. 2, pp. 54–65, March 2014.

[8] J. W. Simpson-Porco, F. Dörfler, and F. Bullo, "Voltage stabilization in microgrids via quadratic droop control," *IEEE Transactions on Automatic Control*, vol. 62, pp. 1239–1253, March 2017.

[9] T. L. Vu and K. Turitsyn, "A framework for robust assessment of power grid stability and resiliency," *IEEE Transactions on Automatic Control*, vol. 62, pp. 1165–1177, March 2017.

[10] M. Tucci, S. Riverso, and G. Ferrari-Trecate, "Voltage stabilization in dc microgrids through coupling-independent plug-and-play controllers," in *2016 IEEE 55th Conference on Decision and Control (CDC)*, pp. 4944–4949, Dec 2016.

[11] E. D. Sontag, *Input to State Stability: Basic Concepts and Results*, pp. 163–220. Berlin, Heidelberg: Springer Berlin Heidelberg, 2008.

[12] D. Olivares, A. Mehrizi-Sani, A. Etemadi, C. Canizares, R. Iravani, M. Kazerani, A. Hajimiragha, O. Gomis-Bellmunt, M. Saeedifard, R. Palma-Behnke, G. Jimenez-Estevez, and N. Hatziargyriou, "Trends in microgrid control," *Smart Grid, IEEE Transactions on*, vol. 5, pp. 1905–1919, July 2014.

[13] A. Iovine, G. Damm, E. De Santis, and M. D. Di Benedetto, "Management Controller for a DC MicroGrid integrating Renewables and Storages," in *20th IFAC World Congress on International Federation of Automatic Control (IFAC 2017)*, (Toulouse, France), 2017.

[14] N. Mohan, T. M. Undeland, and W. P. Robbins, *Power electronics*. Wiley, 2003.

[15] P. Kundur, N. J. Balu, and M. G. Lauby, *Power system stability and control*. McGraw-Hill, 1994.

[16] H. K. Khalil, *Nonlinear systems*. Prentice Hall, 2002.